

Utah State University

DigitalCommons@USU

Physics Student Research

Physics Student Research

12-2014

Effects of Major Sudden Stratospheric Warmings Identified in Midlatitude Mesospheric Rayleigh-Scatter Lidar Temperatures

Leda Sox

Utah State University

Vincent B. Wickwar

Utah State University

Chad Fish

ASTRA

Josh Herron

Utah State University

Follow this and additional works at: https://digitalcommons.usu.edu/phys_stures



Part of the [Atmospheric Sciences Commons](#), and the [Atomic, Molecular and Optical Physics Commons](#)

Recommended Citation

Sox, Leda; Wickwar, Vincent B.; Fish, Chad; and Herron, Josh, "Effects of Major Sudden Stratospheric Warmings Identified in Midlatitude Mesospheric Rayleigh-Scatter Lidar Temperatures" (2014). *Physics Student Research*. Paper 14.

https://digitalcommons.usu.edu/phys_stures/14

This Poster is brought to you for free and open access by the Physics Student Research at DigitalCommons@USU. It has been accepted for inclusion in Physics Student Research by an authorized administrator of DigitalCommons@USU. For more information, please contact digitalcommons@usu.edu.



From the SelectedWorks of Leda Sox

December 2014

Effects of Major Sudden Stratospheric Warmings Identified in Midlatitude Mesospheric Rayleigh-Scatter Lidar Temperatures

Contact
Author

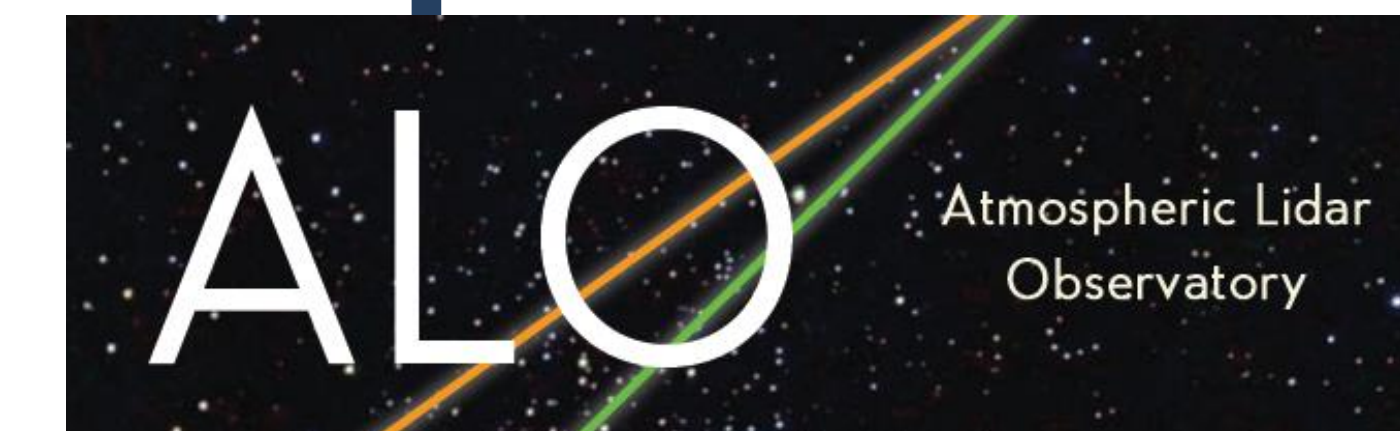
Start Your Own
SelectedWorks

Notify Me
of New Work



Effects of Major Sudden Stratospheric Warmings Identified in Midlatitude Mesospheric Rayleigh-Scatter Lidar Temperatures

Leda Sox¹, Vincent B. Wickwar¹, Chad Fish² and Josh P. Herron²



¹Department of Physics and Center for Atmospheric and Space Sciences, Utah State University, Logan, Utah; ² Space Dynamics Lab, Utah State University, Logan, Utah

Introduction

Sudden Stratospheric Warmings (SSWs) are major disturbances in the polar region of the winter hemisphere that are defined by major changes in stratospheric temperature and circulation. SSWs are characterized by a temperature increase of tens of degrees Kelvin, averaged over 60°-90° latitude, and a weakening of the polar vortex that persists for the order of a week at the 10 hPa level (roughly 32 km) [Labitzke and Naujokat, 2000]. Polar vortices are cyclones centered on both of the Earth's poles that are

present throughout the stratosphere. Strong eastward zonal winds define the polar vortices in the winter. Increased planetary wave (PW) activity in the winter hemisphere leads to increased PW breaking in the polar stratosphere and the deposition of the PW's westward momentum in the polar vortex. This weakens the polar vortex, and in the case of major SSWs, can reverse the zonal wind direction to westward. The reversal of the stratospheric jet allows more eastward propagating gravity waves (GWs) to travel up into

the mesosphere where, under normal winter conditions, westward propagating GWs dominate. The atypical wintertime GW filtering and the resulting dominance of westward GWs induce an equatorward circulation in the mesosphere, similar to what it is in summer, which leads to the cooling of the upper mesosphere. While these mesospheric coolings have been observed in the polar regions for several decades [Labitzke, 1972], they have only recently been observed at midlatitudes [Yuan *et al.*, 2012].

1. SSWs and USU Rayleigh Lidar Temperatures from 1993-2004

In this study of the mesosphere's response to SSWs above Logan, UT, we will focus on periods when there were major SSW events during the Utah State University Rayleigh-Scatter Lidar's (RSL's) original operational run (Table 1). A major SSW is characterized by both a stratospheric temperature increase averaged over the latitudes 60° and poleward at 10 hPa and a complete reversal of the zonal-mean zonal winds from eastward to westward at 60° and 10 hPa (as seen in NASA's Modern-Era Retrospective Analysis for Research and Applications reanalysis dataset [NASA MERRA]). This creates a complete change in the circulation, or a breakdown, of the polar vortex [Labitzke and Naujokat, 2000]. Two major Northern hemisphere SSWs (one in December and one in January) can be seen in Figure 1 (a) and (b), where they are each denoted by a vertical blue line.

The original RSL system ran at a midlatitude site (41.7° N, 111.8° W), on the campus of USU, from 1993-2004. The RSL measured relative densities that were then used in the Chanin-Hauchecorne method [Hauchecorne and Chanin, 1980], which uses hydrostatic equilibrium and the ideal gas law to give absolute temperatures. The initial temperature values for the downward integration came from the Colorado State University's climatology [She *et al.*, 2000]. The 11 year's worth of temperatures were averaged together with a 31-day sliding window to create a mesospheric temperature climatology [Herron, 2007]. Winter and summer months are shown in Figure 2.

SSW Event	Peak Date	Nights of Data
Jan-Feb 1995	05 Feb '95	18
Dec 1998- Jan 1999	15 Dec '98	16
Feb-Mar 1999	26 Feb '99	19
Mar-Apr 2000	20 Mar '00	9
Jan-Mar 2001	11 Feb '01	33
Jan-Feb 2003	18 Jan '03	18

Table 1. List of major SSWs, their peak dates (when zonal wind direction reversed), and the nights of RSL data from 1993-2004

2. Midlatitude Mesospheric Temperatures during SSWs

Of the 10 winters during the USU RSL observational run, there were 7 major SSWs. RSL temperature data were obtained during 6 of these major SSWs (Table 1). In Figure 3 (a-f), the RSL temperatures are plotted during the 6 SSW event periods. The red vertical lines in the plots give the peak date, which is defined as the date when the zonal-mean zonal winds reversed directions according to MERRA data. The RSL observations show a temperature range of 180–260 K, from high-to-low altitudes, prior to the peak date and a range of 160–280 K after the peak date.

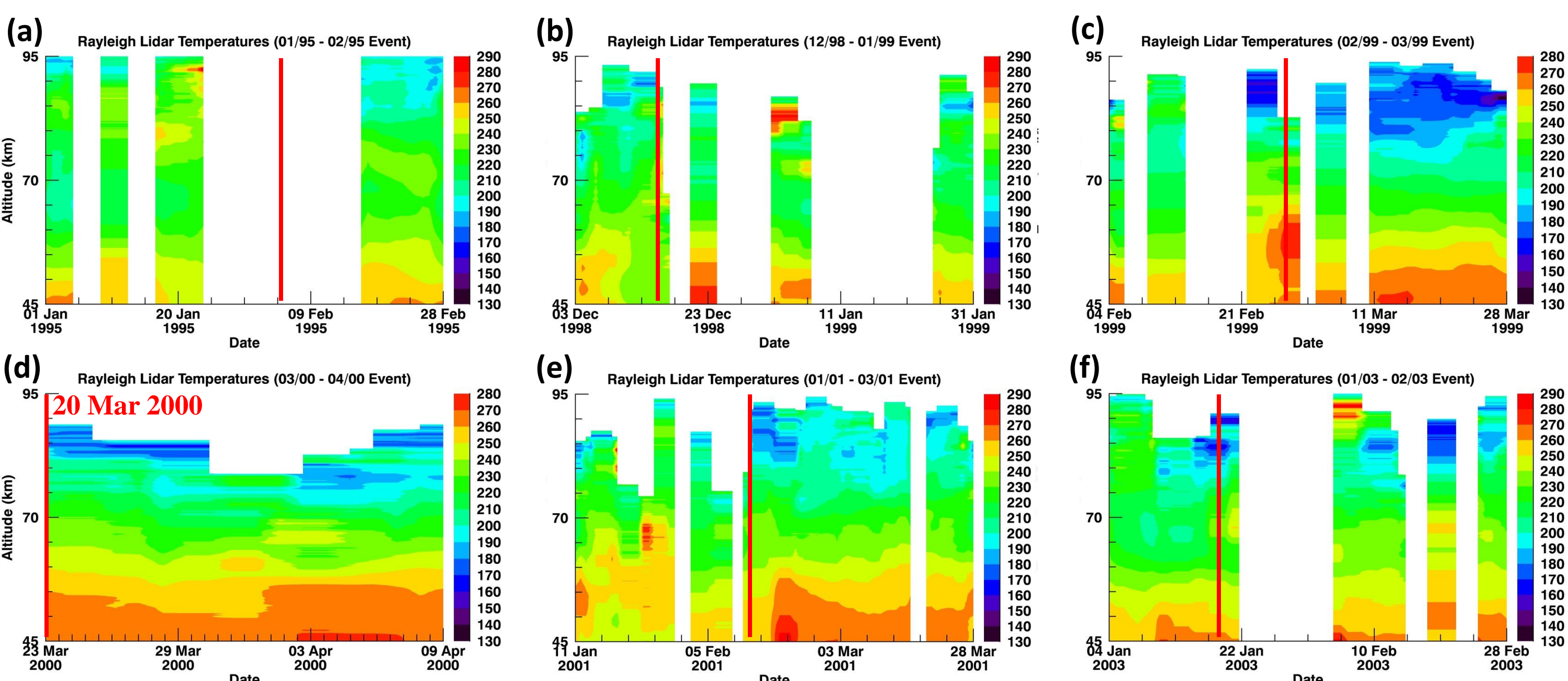


Figure 3. USU Rayleigh Lidar mesospheric temperatures during six (a-f) major sudden stratospheric warmings that occurred from 1993-2004. The red vertical lines indicate peak dates of the SSW event. Plots a-f refer to the SSW events given in Table 1.

The RSL mesospheric temperature range prior to the SSW peak dates is similar to that of the climatological winter temperature range (Figure 2a), as expected. Whereas, after the peak date, the RSL mesospheric temperature range switches to a range more similar to that of the climatological summer temperature range (Figure 2b). This winter-to-summer temperature reversal starts near the peak date and continues for several weeks afterward

Conclusions and Future Work

In this work, we present a study of the behavior of the mesosphere, from a midlatitude Rayleigh lidar site, during six major sudden stratospheric warmings. Our conclusions include:

- A dense temperature dataset, acquired by the USU Rayleigh lidar, overlaps significantly with nearly all of the major SSW events from 1993-2004
- The observed midlatitude mesosphere, from 45-90 km, undergoes a winter-to-summer temperature reversal from the time of the stratospheric zonal wind reversal at 60 N.
- The mesospheric temperature anomalies, coolings in the upper mesosphere and warmings in the lower mesosphere, are roughly the same magnitude at midlatitudes as they are in the polar regions.

This work will be furthered by examining the behavior of the midlatitude lower thermosphere in future observations with the recently upgraded USU RSL, which now has an observational range of 70-114 km [Wickwar *et al.*, 2014].

References

Hauchecorne, A. and M. L. Chanin (1980), Density and temperature profiles obtained by lidar between 35 and 70 km, *Geophys. Res. Lett.*, 7, 565–568.
Herron, J. P. (2007), Rayleigh-Scatter Lidar Observations at USU's Atmospheric Lidar Observatory (Logan, UT) — Temperature Climatology Comparisons with MSIS, and Noctilucent Clouds, PhD Dissertation, Utah State University, Logan, UT, pp156.
Labitzke, K. (1972), Temperature changes in the mesosphere and stratosphere connected with circulation changes in winter, *J. Atmos. Sci.*, 29, 756–766.
Labitzke, K., and B. Naujokat (2000), The lower arctic stratosphere in winter since 1952, *SPARC NewsL.*, 15, 11–14.
Liu, H.-L., and R. G. Roble (2002), A study of a self-generated stratospheric sudden warming and its mesospheric-lower thermospheric impacts using the coupled TIME-GCM/CCM3, *J. Geophys. Res.*, 107 (D23), 4695, doi:10.1029/2001JD001533.

NASA MERRA Database Website: http://acd-ext.gsfc.nasa.gov/Data_services/met/ann_data.html
She, C. Y., S. Chen, Z. Hu, J. Sherman, J. D. Vance, V. Vasoli, M. A. White, J. R. Yu, and D. A. Krueger (2000), Eight-year climatology of nocturnal temperature and sodium density in the mesopause region (80 to 105 km) over Fort Collins, CO (41 N, 105 W), *Geophys. Res. Lett.*, 27, 3289-3292.
Yuan, T., B. Thuraiaraj, C.-Y. She, A. Chandran, R. L. Collins, and D. A. Krueger (2012), Wind and temperature response of midlatitude mesopause region to the 2009 Sudden Stratospheric Warming, *J. Geophys. Res.*, 117, D09114, doi:10.1029/2011JD017142.
Wickwar, V. B., et al. (2014), A Lidar for the Region from the Stratosphere to the Thermosphere. American Geophysical Union Fall Meeting, S441C-4078

3. Mesospheric Temperature Differences during SSWs

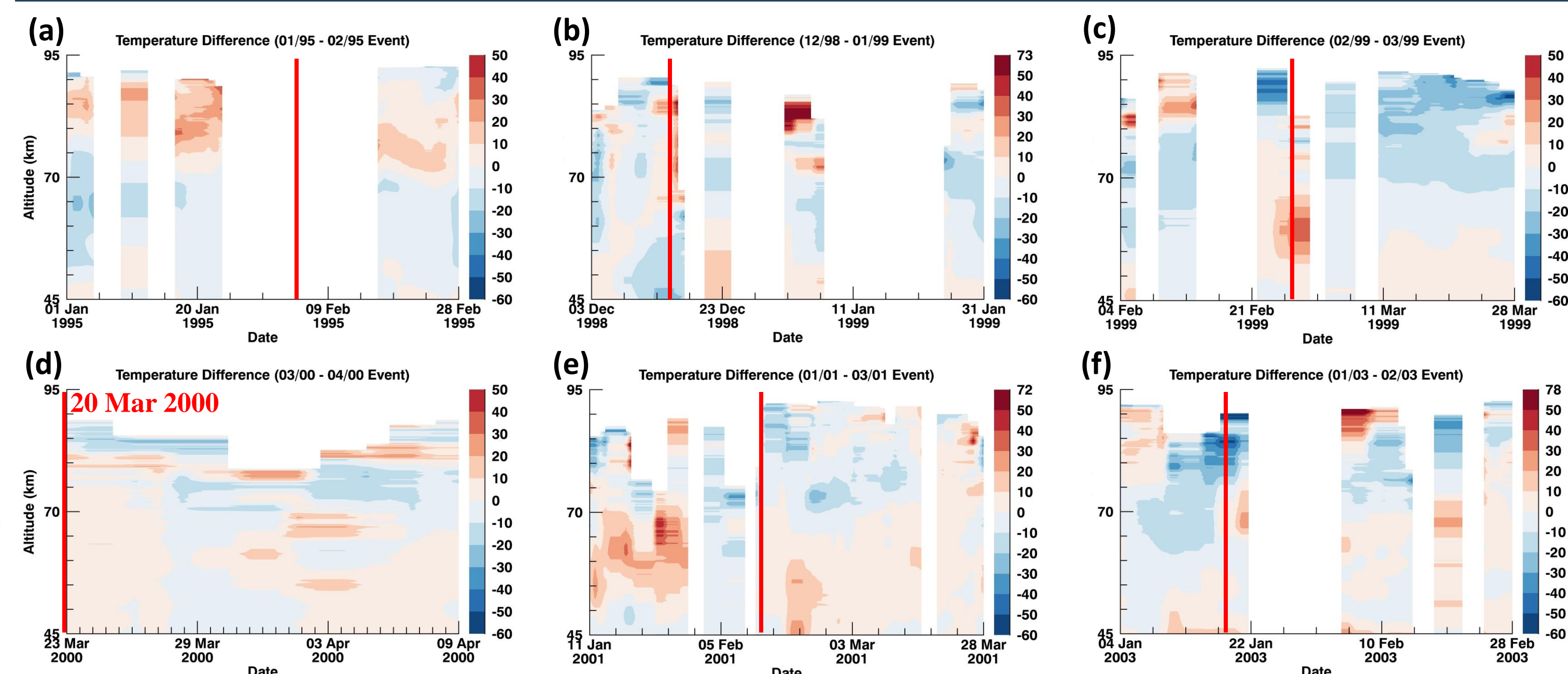


Figure 4. Mesospheric Temperature differences between climatological and night-average values during the six (a-f) major SSWs from 1993-2004. Red vertical lines indicate the peak dates of the major SSWs.

In order to better define coolings and warmings during an SSW event, temperature difference plots (Figure 4) were created by subtracting the RSL climatological night's temperatures (Figure 2a) from the individual night's averaged temperatures (Figure 3). The observed upper mesospheric coolings, that are typically located from 70-95 km, and lower mesospheric warmings, from 45-70 km, are roughly one order of magnitude higher than those predicted in Liu and Roble, [2002] for midlatitudes. They are more comparable to the coolings and warmings that have been found in the polar mesosphere [Labitzke, 1972] and range from less than –50 K (coolings) to more than +50 K (warmings).

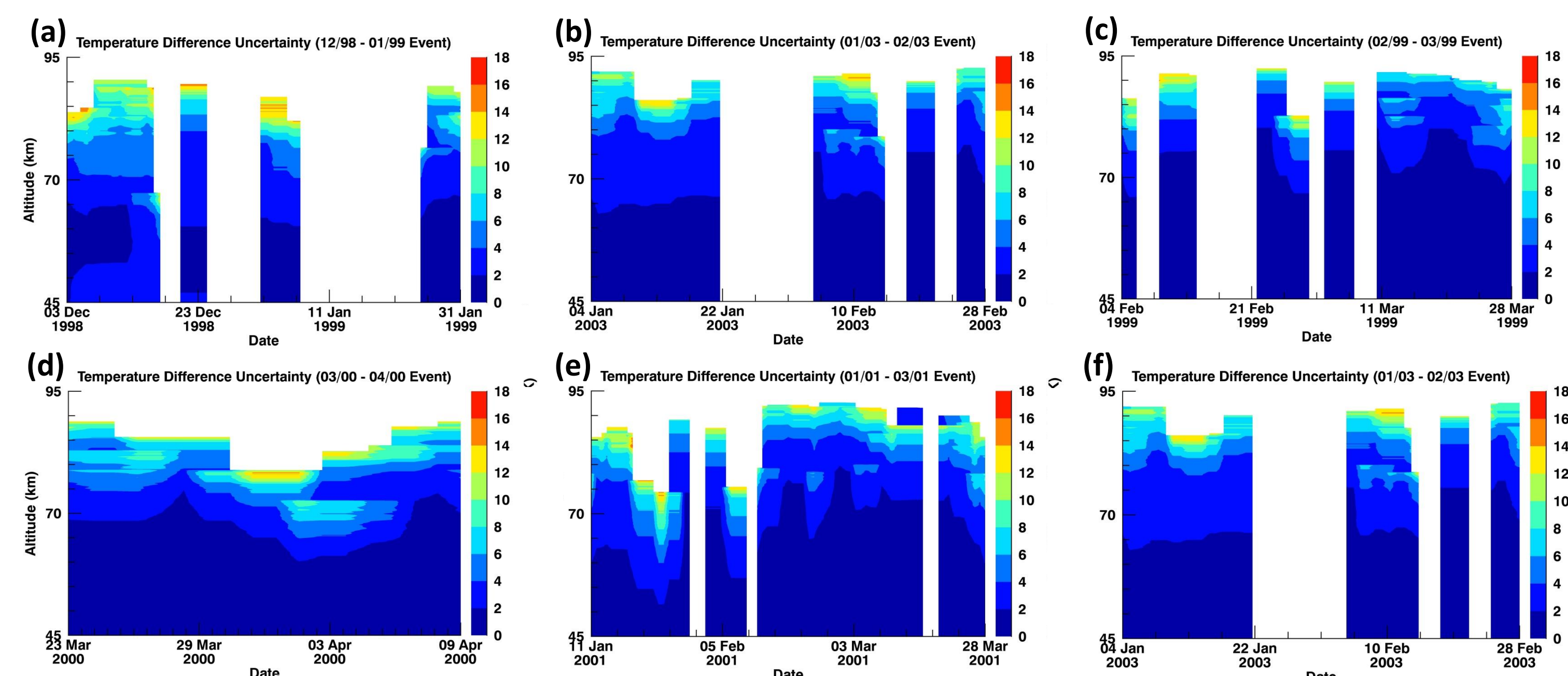


Figure 5. Uncertainty in the mesospheric temperature differences during the six (a-f) major SSWs from 1993-2004.

Figure 5 (a-f) gives the uncertainty of the temperature difference calculation, from Figure 4, which is defined as:

$$\sigma_{D_i} = \sqrt{\sigma_{N_i}^2 + \sigma_{\bar{C}_i}^2}$$

Where σ_{D_i} is the uncertainty in the temperature difference, at each altitude, i , σ_{N_i} is the uncertainty in an individual night's temperatures based on Poisson statistics, at each altitude, i , and $\sigma_{\bar{C}_i}$ is the uncertainty of the mean in a climatological night's temperatures based on Poisson statistics and geophysical variability, at each altitude, i . The uncertainty versus height plots (Figure 5) show that the warmings at the lowest altitudes and the coolings at the highest altitudes in Figure 4 are significant.

Acknowledgments

Leda Sox would like to acknowledge financial support from USU, the Utah NASA Space Grant Consortium, and the USU Physics Department's Blood Scholarship and Gene Adams Scholarship. The data were acquired with support from several grants from the Atmospheric Sciences Division of the National Science Foundation.